Available online at www.sciencedirect.com

ScienceDirect

journal homepage: www.elsevier.com/locate/he

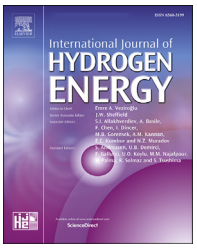

Data-driven fault diagnosis for PEMFC systems of hybrid tram based on deep learning

Xuexia Zhang[*], *Jingzhe Zhou*, *Weirong Chen*

School of Electrical Engineering, Southwest Jiaotong University, Chengdu 611756, China

HIGHLIGHTS

- Selecting the fault diagnosis sample by SAGAFCM algorithm.
- Processing the unbalanced data by SMOTE algorithm.
- Using DBN for the fault diagnosis of the PEMFC system and obtaining a good result.

ARTICLE INFO

Article history:
Received 2 December 2019
Received in revised form
3 March 2020
Accepted 6 March 2020
Available online xxx

Keywords:
Deep brief learning
Fault diagnosis
Hybrid tram
PEMFC systems
Synthetic minority over-sampling technique
Simulated annealing genetic algorithm fuzzy c-means clustering

ABSTRACT

The running state of the hybrid tram and the service life of fuel cell stacks are related to the fault diagnosis strategy of the proton exchange membrane fuel cell (PEMFC) system. In order to accurately detect various fault types, a novel method is proposed to classify the different health states, which is composed of simulated annealing genetic algorithm fuzzy c-means clustering (SAGAFCM) and deep belief network (DBN) combined with synthetic minority over-sampling technique (SMOTE). Operation data generated by the tram are clustered by SAGAFCM algorithm, and valid data are selected as fault diagnosis samples which include the training sample and the test sample. However, the fault samples are usually unbalanced data. To reduce the influence of unbalanced data on the fault diagnosis accuracy, SMOTE is employed to form a new training sample by supplementing the data of the small sample. Then DBN is trained by the new training sample to obtain the fault diagnosis model. In this paper, the proposed method can well distinguish the four health states, which are high deionized water inlet temperature fault, hydrogen leakage fault, low air pressure fault and the normal state, with an accuracy of 99.97% for the training sample and 100% for the test sample.

Introduction

Fuel cells are clean, efficient, and sustainable, and proton exchange membrane fuel cell (PEMFC) has the extra merits of high-power density, shorter start-up time, fast response speed, low operating temperature, and no leakage of electrolytes, which give it a broad application prospect [1,2]. However, for the further commercial development of PEMFC, durability and sustainability are two key issues [3,4]. Nowadays, many studies on the fault performance of PEMFC have been proposed. Some three-dimensional simulation models are built to analyze the fault state of PEMFC [5,6]. And more detailed measurement techniques, such as Electrochemical Impedance Spectroscopy (EIS), are used to diagnose the

* *Corresponding author.*
E-mail addresses: survival_zxx@sina.com (X. Zhang), Jingzhez123@163.com (J. Zhou), wrchen@swjtu.edu.cn (W. Chen).
https://doi.org/10.1016/j.ijhydene.2020.03.035
0360-3199/

Nomenclature

BiLSTM	bidirectional long short-term memory
DBN	deep belief network
DHMM	discrete hidden Markov model
EIS	electrochemical impedance spectroscopy
FCM	fuzzy c-means clustering
FDI	fault detection and isolation
FDA	fisher discriminative analysis
GA	genetic algorithm
LDA	linear discriminant analysis
PEMFC	proton exchange membrane fuel cells
SVM	support vector machine
SSM-SVM	sphere shaped multiclass support vector machine
RC	reservoir computing
SMOTE	synthetic minority over-sampler technique
SA	simulated annealing
t-SNE	t-distributed stochastic neighbor embedding
SSAEs	stacked sparse autoencoders
VSS	voltage singularity spectrum
a	bias vector of the visible layer
b	bias vector of the hidden layer
v	state vector of the visible layer
h	state vector of the hidden layer
f	fitness function
α	cooling rate
C	clustering center vector
J	objective function
N	sampling rate
T_0	Initial temperature
T_n	termination temperature
U	membership matrix
W	weight matrix

performance of high-power PEMFC system and to monitor the impedance spectrum of PEMFC system online [7,8]. Reference [9] introduces a method that can quickly estimate the impedance of a fuel cell by using two high-bandwidth and short-time signals with different phases. In addition to the faults of PEMFC stacks, the sensor faults are distinguished from the faults of the stacks [10,11]. In Refs. [12], delayed Linear Parameter Varying system observer is used to diagnose the actuator faults of PEMFC. The faults occurred during the actual operation can lead to the performance degradation and irreversibly damage of fuel cells. Therefore, in order to ensure the normal operation of the system, fault diagnosis can be seen an effective measure to isolate and correct the fault in time, and fault diagnosis technology has received more and more attention in the field of PEMFC [13,14].

The fault diagnosis methods proposed generally include model-based fault diagnosis methods and non-model based fault diagnosis methods [15,16]. Model-based methods usually establish a mathematical or physical model to simulate the physical phenomenon in the normal operation, and residuals are generated by comparing the simulated results with those measured on the real systems [17]. Reference [18] proposes a model-based fault diagnosis method based on structural analysis and causal computation theories to classify nine different faults in the automotive PEMFC system. Although many methods about establishing impedance model and equivalent circuit model for the fault diagnosis of PEMFC are proposed [19,20], the fuel cell system is a very complicated, nonlinear, and strong coupling system which involves the fields of electrochemistry, thermodynamics, material, machinery and so on, the accurate mechanical model of it is difficult to obtain. Therefore, non-model based fault diagnosis methods are widely used [21]. Reference [22] developes an online non-invasive diagnostic tool, which combined wavelet transform-based multifractal formalism and pattern recognition methods to identify multiple fault states of PEMFC systems. In addition, they use voltage singularity spectrum (VSS) and machine learning framework to classify the faults of two different stacks (automotive applications and stationary use), and the results show that this method can identify more complex faults combining multiple fault types [23]. Most of non-model based fault diagnosis methods are data-driven fault diagnosis methods which can analyze the massive data and get fault diagnosis result without knowing the precise analytical model of the system. Reference [24] proposes a double-fuzzy diagnostic method combining EIS, which can identify the oxygen saturation state, normal state, and the oxygen hunger state of a 2 kW fuel cell system online, with a classification rate of 100%. Reference [25] proposes an off-line data-driven fault detection and isolation (FDI) system for solid oxide fuel cell stack by support vector machine (SVM) classifier. And the result proves that data-driven system is more adoptable. In Ref. [26,27], principal component analysis (PCA) is used for feature extraction, proving that this method can improve the accuracy of fault diagnosis. At present, SVM method is widely used in the field of the data-driven fault diagnosis. Reference [28] employes the algorithm of fisher discriminate analysis (FDA) and SVM to process the voltage signal of a single fuel cell. And they also develop a highly integrated electronic chip to realize the multi-fault online diagnosis of PEMFC stacks. Reference [29] considers dynamic behaviors and spatial inhomogeneity of the PEMFC system at the same time. They use a time-series analysis tool to extract features from the single cell voltage signals. In addition, the fault diagnosis of five health states is achieved by using the classification tool named sphere shaped multiclass support vector machine (SSM-SVM) with 96.13% diagnostic accuracy. In Ref. [30], they use SSM-SVM and linear discriminant analysis (LDA) to extract the characteristics of the magnetic field data obtained by magnetic field sensors installed around the PEMFC stacks based on non-invasive magnetic measurement, and fault identification of seven health states are realized with 98.26% diagnostic accuracy. Reference [31] uses relevance vector machine (an improved method based on SVM) and orthogonal linear discriminant analysis to realize the online adaptive water management fault diagnosis of PEMFC. These methods have shown good results in the fault diagnosis of PEMFC stacks, but they are mostly faced with small samples of data. For the fuel cell systems of tram, reference [32] proposes a fault diagnosis method based on discrete hidden Markov model (DHMM) and k-means fuzzy clustering to classify six kinds of faults, reaching an accuracy of 94%. Although the

Please cite this article as: Zhang X et al., Data-driven fault diagnosis for PEMFC systems of hybrid tram based on deep learning, International Journal of Hydrogen Energy, https://doi.org/10.1016/j.ijhydene.2020.03.035

classification of normal state is not accurate, the total accuracy is improved compared with the SVM method. However, the sample in this reference is small and ideal, whereas for the fuel cell systems of tram, fault diagnosis with large samples is necessary.

Nowadays, neural network and deep learning have developed rapidly and been extensively used in fault diagnosis field. Reference [33] first introduces the reservoir computing (RC) method in the field of fuel cell diagnosis, which is simulated by a special kind of virtual neural network with complex dynamics modeled by nonlinear time-delay equation. They apply a brain-inspired computational method for RC to classify four health states of PEMFC with an excellent classification accuracy of 99.88% for offline training process and 92.43% for the new data. Reference [34] proposes a method combined of the bidirectional long short-term memory (BiLSTM)) network and t-distributed stochastic neighbor embedding (t-SNE) for sequence failure diagnosis of the PEMFC water management subsystem. t-SNE is first applied to feature extraction and then BiLSTM is used for fault diagnosis. The accuracy of fault diagnosis reaches 96.88%. Reference [35] proposes an innovative and intelligent diagnosis method based on stacked sparse autoencoders (SSAEs), which can solve the simultaneous fault problem by using only 16 measurement values.

The above methods basically depend on the analysis of small samples, and the shortcomings show up when analyzing large sample data by these methods. Nowadays, with the advent of the big data era, the fault diagnosis methods of PEMFC need to analyze massive data. And deep learning has obvious advantages in analyzing massive data. Deep belief network (DBN) is proposed by Geoffrey Hinton in 2006 [36]. At present, DBN is already well established in many fields such as handwritten digit recognition, speech recognition, image recognition and machine translation [37–39]. However, DBN is not widely applied in the field of fault diagnosis. And most of these applications are in mechanical fault diagnosis field [40,41]. For instance, Refs. [42,43] apply the improved DBN to bearing fault diagnosis. Reference [44] proposes a hybrid deep belief network (HDBN) learning model for intelligent fault diagnosis of motor drive systems such as automobile drive systems. DBN adopts an unsupervised approach to network parameters pre-training, which is conducive to the network parameter initialization approaching the global optimal solution. Reference [45] establishes a DBN fault diagnosis model and compares it with BP neural network, SVM, self-organizing mapping network, and genetic algorithm. The results show that DBN is obviously superior to other methods. These studies show that DBN has a good effect when analyzing big data in fault diagnosis. Currently, DBN has not been applied to PEMFC fault diagnosis.

In order to study the fault diagnosis methods in large sample data of PEMFC, the application of DBN in fault diagnosis of PEMFC system for tram is proposed for the first time in this paper. Normalization and PCA are used to preprocess the selected original data. And due to the redundant and invalid data in the collected original data, simulated annealing genetic algorithm fuzzy c-means clustering (SAGAFCM) is used to screen the fault samples from the original data. However, the fault samples of PEMFC are usually unbalanced data, which can reduce the accuracy of the fault classification. Thus, in this paper, synthetic minority over-sampling technique (SMOTE) is employed to complement the small sample before the training of DBN. Through this method, the accuracy of fault diagnosis can be effectively increased.

This paper is organized as follows: Section Data source introduces the data source of this study, including the introductions to the fuel cell system and the fault types. In Section Diagnosis approach, the principles of the main algorithms employed in this study are briefly introduced. And the process of fault diagnosis is presented in Section Fault diagnosis based on SAGAFCM and DBN combined with SMOTE. Following that, the results and discussion are provided in Section Results and discussions. Finally, the paper is concluded in Section Conclusions.

Data source

Introduction to fuel cell system of the tram

In April 2016, our group successfully developed the world's first commercial hydrogen fuel cell hybrid 100% low floor tram (see Fig. 1) in cooperation with Tangshan Tramcar [46]. And the main parameters of the tram are shown in Table 1 [47]. In this paper, the original data are all from the operation data of this tram.

The fuel cell module of the tram is composed of PEMFC stacks, air supply system, hydrogen supply system, cooling system, cooling circulation system, and hydrogen circulation system [32]. And two 150 kW FC velocity-HD6 PEMFC modules (see Fig. 2) are used in the system. The parameters of the stacks are shown in Table 2.

Fault classifications

When the HD6 is in a fault state, a digital signal will be output, and the current active fault and the corresponding severity level will be reflected in the bus through the system. In this system, the fault of the fuel cell module is divided into four severity levels, including level 0 warning state, level 1 alarm state, level 2 alarm state and level 3 alarm state. And the definition is shown in Table 3. Once the system enters the fault alarm state of level 2 or level 3, the request current signal and the actual current value will change to 0, and the tram will immediately enter the fault shutdown mode which means that the fuel cell module will no longer operate. Only after the fault is solved, the stacks can be restarted. Thus, for the normal operation of the tram, detecting and eliminating the level 1 alarm fault in time is necessary to prevent the fuel cell system from entering into a more advanced fault.

Introduction to fault types

For effective control of the tram PEMFC system, the faults of severity level 1 should be detected in time. Therefore, in this paper, several level 1 faults are focused on as follows:

High deionized water inlet temperature fault: High deionized water inlet temperature fault means the fault warning when the inlet temperature of deionized glycol is higher than

Please cite this article as: Zhang X et al., Data-driven fault diagnosis for PEMFC systems of hybrid tram based on deep learning, International Journal of Hydrogen Energy, https://doi.org/10.1016/j.ijhydene.2020.03.035

Fig. 1 – The world's first commercial hydrogen fuel cell hybrid tram.

Table 1 – Parameters of the tram.

Technical Indicators	Parameters
Fuel cell types	PEMFC
Fuel cell power	300 kW
Hydrogen storage mode	High Pressure Hydrogen Tank
Hydrogen storage pressure	35 MPa
Body length	37 m
Vehicle weight	52 t
Power supply voltage	750 VDC
Maximum operating speed	70 km/h
Passenger capacity	354

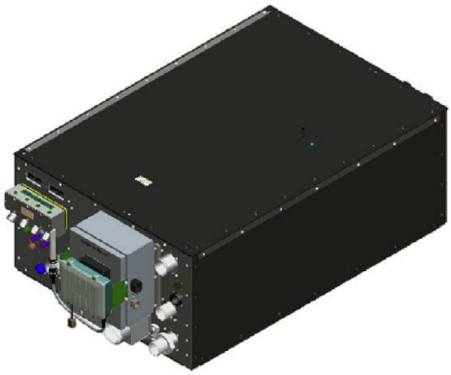

Fig. 2 – HD6 PEMFC module.

Table 2 – Parameters of the fuel cell stacks.

Names	Parameters
Weight	404 Kg
Volume	1530 mm × 871 mm × 495 mm
Rated power	150 kW
Working voltage	465 – 730 V
Maximum working current	300 A
Fuel	Hydrogen
Oxidant	Air
Coolant	Water and glycol
Coolant temperature (nominal)	63 °C
Minimum fuel pressure	16 Bar

Table 3 – Descriptions of the fault severity levels.

Severity level	Description
0: Info	• No reporting to drive the system. • No system reaction. • For information only.
1: Warning	• A system parameter has exceeded normal range. • The hardware fuel cell module fault digital output remains unchanged (active). • Fuel cell module output power may be reduced while the fault is active. • The module should be inspected and/or process data reviewed does not result in a shutdown.
2: Alarm	• A system parameter has exceeded the acceptable operating range, and the fuel cell module will shut down. • The hardware fuel cell module fault digital output switches to faulted (deactivated = 0 V). • After a severity 2 fault, one module restart can be attempted to clear the fault and continue operation. • If there is a subsequent severity 2 fault, do not attempt a restart until action has been taken to identify and resolve the cause of the fault.
3: Severe alarm	• A system parameter has exceeded a safe operating range, and the fuel cell module must be immediately shut down. • The fuel cell module will immediately enter Faulted State. And the hardware fuel cell module fault digital output switches to faulted (deactivated = 0 V). • After a severity 3 fault, the fuel cell module must not be restarted until the cause of the fault has been determined, and resolved. In addition, the module should be inspected for safe operation.

68 °C. As for the causes, air in the fuel cell cooling system, cooling system fault, and the corresponding pressure sensor fault are all likely to cause this fault. Generally, checking coolant bleed port, air cooling system, cooling system operation, and pressure sensor functionality or wiring can repair the fault.

Hydrogen leakage: Hydrogen leakage fault will occur when the hydrogen sensor value is more than 2%, which means the hydrogen reactant in the fuel cell reaction site is not enough. In severe case, hydrogen combustion or hydrogen explosion may be caused when the volume concentration of the mixture of hydrogen and oxygen reaches 4%–75%. Actually, hydrogen

Please cite this article as: Zhang X et al., Data-driven fault diagnosis for PEMFC systems of hybrid tram based on deep learning, International Journal of Hydrogen Energy, https://doi.org/10.1016/j.ijhydene.2020.03.035

leakage may be caused by many reasons, such as faults in purge valve, air system, fuel cells hydrogen internal transfer device, and the corresponding pressure relief valve. Generally, this fault can be repaired by checking the purge valve operation, checking the air system operation, testing the module transfer device.

Low air pressure: Low air pressure cannot guarantee the continuous oxygen supply to the stack, which may be caused by the low oxygen flow. When the oxygen supply is insufficient to the stack, the output voltage of the stack will be rapidly attenuated. And "hot spots" will appear on the membrane surface, which can reduce the service life of the stack. The low air pressure fault may be caused by module air supply system fault, back pressure valve fault, air bypass valve fault, or exhaust blockage. And checking air supply system operation, back pressure valve, air bypass valve operation, and whether exhaust can avoid this fault.

Diagnosis approach

In this paper, one of the emphases of the fault diagnosis method is to select the fault samples from the original data by the SAGAFCM clustering algorithm. And another emphasis is to use DBN combined with SMOTE for fault diagnosis by the fault samples.

Simulated annealing genetic algorithm fuzzy c-means clustering

The concept of membership degree is introduced in fuzzy c-means clustering (FCM) algorithm, which is beneficial to choose the required data [48]. However, the performance of the traditional FCM algorithm depends on the initial clustering center, which makes the result easy to fall into the local optimal solution [49]. To address this problem, simulated annealing genetic algorithm (SAGA) is combined with FCM in this paper. And the process of SAGAFCM is shown in Fig. 3. Through this method, an optimal initial clustering center of FCM and a better cluster result can be obtained.

FCM: FCM is a fuzzy clustering method based on objective function minimization [50]. Compared with other traditional clustering methods, FCM method is more flexible in partitioning data. In other words, each cluster generated by FCM is regarded as a fuzzy set. And the evaluation result is not fixed, while the probability of the data belonging to each cluster is obtained through the membership matrix.

The definition of the objective function J of FCM is shown in Equation (1), and the constraint condition is shown in equation (2).

$$J = \sum_{i=1}^{c}\sum_{j=1}^{n} u_{ij}^{m}\left\|x_j - c_i\right\|^2 \tag{1}$$

$$\sum_{i=1}^{c} u_{ij} = 1, j = 1, 2, \ldots, n \tag{2}$$

where J is the value of the target function, c is the number of clustering categories, n is the number of data, x_j is the position of the data set j, c_i represents the clustering center of category i, u_{ij} is the membership degree of sample j belonging to category i, m is the membership degree factor, indicating the degree of lightness of the sample.

In order to find the minimum value of the objective function J, the membership degree u_{ij} (see equation (3)) of the sample and the clustering center c_i (see equation (4)) are required.

$$u_{ij} = \frac{1}{\sum_{k=1}^{c}\left(\frac{\left\|x_j - c_i\right\|}{\left\|x_j - c_k\right\|}\right)^{\left(\frac{2}{m-1}\right)}} \tag{3}$$

$$c_i = \sum_{j=1}^{n} \frac{u_{ij}^{m}}{\sum_{j=1}^{n} u_{ij}^{m}} x_j \tag{4}$$

Calculation steps of FCM are as follows:

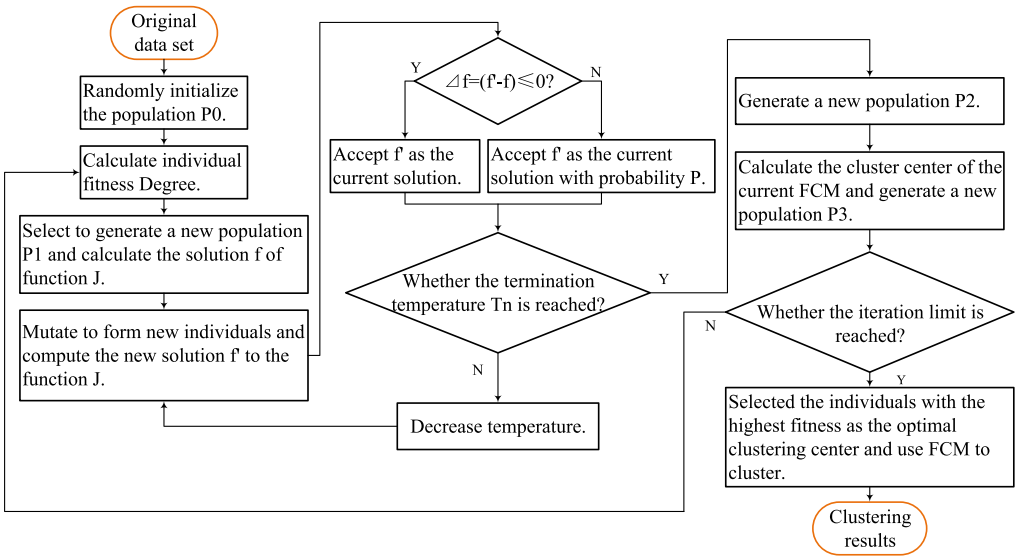

Fig. 3 – Process of SAGAFCM algorithm.

Please cite this article as: Zhang X et al., Data-driven fault diagnosis for PEMFC systems of hybrid tram based on deep learning, International Journal of Hydrogen Energy, https://doi.org/10.1016/j.ijhydene.2020.03.035

(1) Determine the classification number c, membership factor m, number of iterations and end conditions.
(2) Initialize membership matrix $U = [u_{ij}]$.
(3) Calculate clustering center $C = [c_i]$ according to U.
(4) Calculate the value of the objective function J and judge whether the end condition is satisfied.

SAGA: Genetic algorithm (GA) is a global optimized adaptive probabilistic search algorithm, which simulates gene mutation, gene recombination, natural selection, and isolated speciation process of biological population evolution [51]. As an optimization algorithm, it can be employed to find the maximum or minimum value of the function. The main steps of GA are as follows:

(1) Initialization

In this step, the initial population composed of n strings is randomly generated. And the individuals are encoded in the population by generally using binary encoding.

(2) Individual fitness degree evaluation

The individual fitness degree is calculated according to the fitness function J in this step.

(3) Selection

After the individual fitness degree is calculated, the opportunity for each individual to inherit in the next generation is determined. Then the n strings are copied.

(4) Crossover

The copied strings are paired in pairs to intersect with crossover probability.

(5) Mutation

In this step, the gene of each string is flipped according to the mutation probability.

(6) A new population is created.

Although GA has a strong global search capability, this algorithm is prone to premature convergence [52]. Whereas simulated annealing (SA) is an optimization algorithm that simulates the annealing process of high temperature solids [53]. Considering the defect of GA, SAGA is proposed as an improved algorithm. And the process of the algorithm is shown in Fig. 3. Through the improved algorithm, the iterative process of the algorithm is controlled by adding the temperature parameter T on the basis of GA, and the evolutionary process of the algorithm is controlled by using the Metropolis rule [54]. Besides, initial temperature T_0, termination temperature T_n, and the cooling rate α ($\alpha \leq 1$) are set at the beginning. Then the temperature is updated by equation (5) after each iteration.

$$T_{new} = \alpha \bullet T_{old} \tag{5}$$

When new individuals are being selected, the fitness difference value between new and old individuals is calculated by equation (6). Then the probability P is calculated by equation (7).

$$\Delta f = f_{new} - f_{old} \tag{6}$$

$$P = \begin{cases} 1, \Delta f > 0 \\ \exp\left(\frac{\Delta f}{T}\right), \Delta f \leq 0 \end{cases} \tag{7}$$

where f is the fitness function, P is the probability of the old solution being replaced, f_{new} and f_{old} are fitness functions of the new and the old individuals, and T is the current temperature.

Deep belief network combined with synthetic minority oversampling technique

In fact, DBN is the stacking of multiple restricted Boltzmann machines (RBM) [55]. And the structure of a four-layer DBN model is shown in Fig. 4, which is composed of input layer, hidden layer and output layer. In this paper, softmax classifier is adopted as the output layer. Generally speaking, two steps are mainly included in the training process of DBN [56].

(1) Step one: Pre-training

As shown in Fig. 4, the data are entered in the input layer. Then the input layer is taken as the visible layer, while layer-2 is taken as the hidden layer to construct RBM-1 for training. Then layer-2 is taken as the visible layer and layer-3 is taken as the hidden layer to construct RBM2 for training.

The weight matrix between any two connected neurons in RBM is represented by W, indicating the connection strength. And vector $v = (v_1, v_2, \ldots, v_n)^T$ represents the state of the visible layer, vector $h = (h_1, h_2, \ldots, h_m)^T$ represents the state of the hidden layer, vector $a = (a_1, a_2, \ldots, a_n)^T$ represents the bias vector of the visible layer, and vector $b = (b_1, b_2, \ldots, b_m)^T$ represents the bias vector of the hidden layer.

RBM is an energy-based model [57]. And the energy function is shown in equation (8).

$$E(v, h|\theta) = -\sum_{i=1}^{n}\sum_{j=1}^{m} v_j W_{ij} h_i - \sum_{j=1}^{m} b_j h_j - \sum_{i=1}^{n} a_i v_i \tag{8}$$

where W_{ij} is the element of weight matrix W, n is the number of cells in the visible layer, m is the number of cells in the hidden layer, and $\theta = \{W_{ij}, a_i, b_j : 1 \leq i \leq n, 1 \leq j \leq m\}$ is the parameter of the network.

Parameters $\{W, a, b\}$ are updated by the CD-1 method which is shown in Fig. 4. And the training program is illustrated in Table Algorithm [58].

(2) Step two: Fine-tune

Please cite this article as: Zhang X et al., Data-driven fault diagnosis for PEMFC systems of hybrid tram based on deep learning, International Journal of Hydrogen Energy, https://doi.org/10.1016/j.ijhydene.2020.03.035

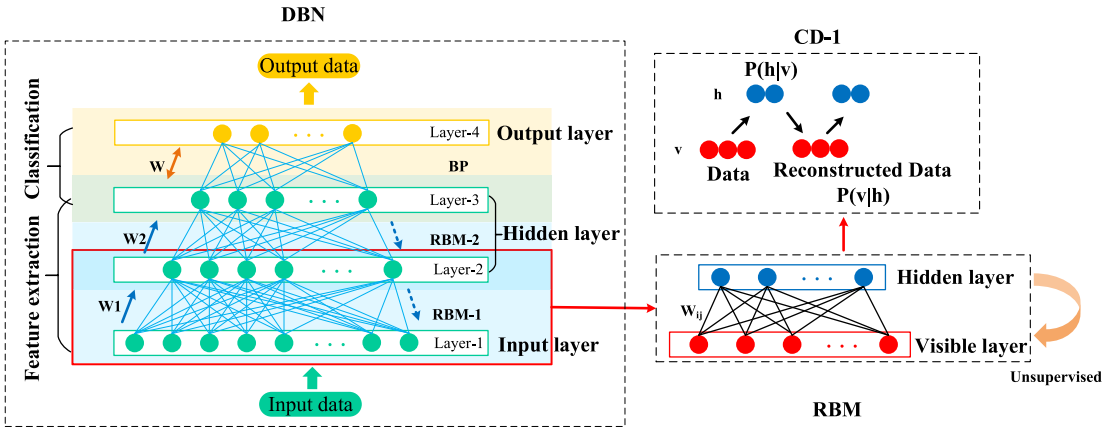

Fig. 4 – Structure of a four-layer DBN.

Algorithm – The training program of RBM

- **Input:** Training sample $x = (x_1, x_2, \ldots, x_n)$, number of hidden layer nodes m, learning rate α, maximum training cycle MAX.
- **Output:** Weight matrix W, visible layer bias vector a, hidden layer bias vector b.
- **Training steps:**(1) Initialization: Set the initial state of visible layer $v_1 = x$, and set the initial value of $\{W, b\}$ to a random small value.

(2) For $t = 1, 2, \ldots, T$
For $j = 1, 2, \ldots, m$
Calculate

$$EP(h_{1j} = 1|v_1) = \sigma(b_j + \sum_i v_{1i} W_{ij}) \quad (9)$$

Take $h_{1j} \in \{0, 1\}$ from the conditional probability $P(h_{1j}|v_1)$.

End For

(3) For $i = 1, 2, \ldots, n$

Calculate

$$P(v_{2i} = 1|h_1) = \sigma(a_i + \sum_j h_{1j} W_{ij}) \quad (10)$$

Take $v_{2i} \in \{0, 1\}$ from the conditional probability

$P(v_{2i}|h_1)$.

End For

(4) For$j = 1, 2, \ldots, m$

Calculate

$$P(v_{2i} = 1|h_1) = \sigma(a_i + \sum_j h_{1j} W_{ij}) \quad (11)$$

End For

(5) Update each parameter according to the follows :

$$W' = W + \varepsilon(P(h_{1.} = 1|v_1)v_1^T - P(h_{2.} = 1|v_2)v_2^T) \quad (12)$$
$$a' = a + \varepsilon(v_1 - v_2) \quad (13)$$
$$b' = b + \varepsilon(P(h_{1.} = 1|v_1) - P(h_{2.} = 1|v_2)) \quad (14)$$

After the training of all RBMs, the backpropagation algorithm (BP) is used to adjust the parameters of all layers which can complete the whole training.

Generally, the amount of diagnosis data varies greatly from one type to another. For such unbalanced samples, the small sample is difficult to be classified accurately by using DBN model only. Therefore, DBN combined with SMOTE is proposed as the fault diagnosis method. Through this method, DBN is trained by the new training sample supplemented by SMOTE algorithm.

In this paper, SMOTE algorithm is mainly used to supplement the data of the small sample. And the steps to synthesize the new samples are as follows [59]:

(1) For each set of data in a small sample s, the Euclidean distance is taken as the standard to calculate the distance to all other data sets in the sample. Then the k nearest neighbors are obtained.
(2) According to the sampling rate N, N sets of data are randomly selected from the k nearest neighbors, denoted as s_j, $j = 1, 2, \ldots, N$.
(3) For the selected neighbor s_j, sample r_j is obtained by random linear interpolation according to equation (15).

$$r_j = s_j + rand(0, 1) \times (s_j - s), j = 1, 2, \ldots, N \quad (15)$$

(4) Sample r_j and s_j are combined to get a new sample s_j'.

Fault diagnosis based on SAGAFCM and DBN combined with SMOTE

The fault diagnosis strategy in this paper is mainly divided into three steps, including the selection of diagnostic variables and original data, data preprocessing, and fault diagnosis. The process is shown in Fig. 5.

Please cite this article as: Zhang X et al., Data-driven fault diagnosis for PEMFC systems of hybrid tram based on deep learning, International Journal of Hydrogen Energy, https://doi.org/10.1016/j.ijhydene.2020.03.035

Selection of diagnostic variables and original data

In order to monitor the running state of the tram, 40 observable variables are monitored. However, only 12 of them can directly reflect the running state of the fuel cell module, because other variables are the parameters of the auxiliary machine running state, the status labels on the device and the trigger signals. Therefore, these 12 variables are selected as the diagnostic variables as shown in Table 4.

According to the 12 diagnostic variables, the operation data of low air pressure fault, high deionized water inlet temperature fault, hydrogen leakage fault, and the normal state are selected as the original data. Then, 1428 sets of normal state data, 230 sets of high deionized water inlet temperature fault data, 65 sets of hydrogen leakage fault data, and 580 sets of low air pressure fault data are obtained. Then the normal state is marked as N1, high deionized water inlet temperature fault is marked as F1, hydrogen leakage fault is marked as F2, and low air pressure fault is marked as F3. Besides, a set of data for each health state is listed in Table 4 as an example.

Table 4 – Diagnostic variables which can directly reflect the running state of the fuel cell and the example sets of data.

Diagnostic variable	Unit	N1	F1	F2	F3
Stack current	A	24.3	24.3	44.5	8.3
Stack voltage	V	697.9	701.2	640.6	692.5
Coolant inlet pressure	MPa	0	0	0.3	0.3
Air inlet pressure	MPa	0.02	0.02	0.43	0.17
Hydrogen pressure at module inlet	MPa	16.6	16.6	16.4	16.9
Hydrogen pressure at stack outlet	MPa	0.45	0.48	0.51	0.25
Hydrogen pressure at stack inlet	MPa	0.53	0.55	0.6	0.3
Air inlet temperature of air compressor	°C	61	61	50	51
Air outlet temperature	°C	64	64	49.5	47.5
Stack coolant outlet temperature	°C	67	67	59.5	59.5
Module coolant inlet temperature	°C	71.5	71	57	58
Stack coolant inlet temperature	°C	72	72	57	58

Data preprocessing

Normalization

As shown in Table 4, the dimensions of the variables vary greatly which can affect the training of the fault diagnosis model, the original data are unified in 0–1 through equation (16) to ensure the reliability of the results [60].

$$x'_i = \frac{x_i - x_{min}}{x_{max} - x_{min}},\ i = 1, 2, \ldots, n \tag{16}$$

where n is the length of the data sequence, x_i is the selected variable, x_{min} is the minimum value of the data sequence, x_{max} is the maximum value of the data sequence, and x'_i is the variable obtained after normalization.

Dimension reduction

In order to reduce computational complexity and improve the visualization effect of the data, PCA is used to convert the correlated variables into several mutually independent variables which can replace the original variables. The essence of PCA depends on diagonalized covariance matrix, which can ensure the data without distortion after dimension reduction to the maximum extent [26]. The principal components (i.e. eigenvectors) of the data and the weights (i.e. eigenvalues) are obtained by eigen decomposition of the covariance matrix, so as to minimize the correlation between the retained dimensions and maximize the variance of the retained dimensions. Therefore, PCA is usually used to reduce the

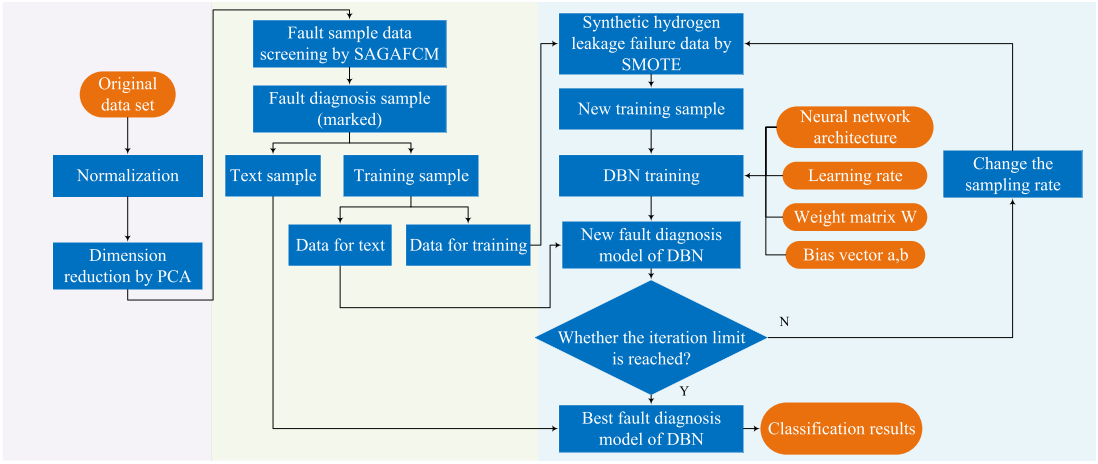

Fig. 5 – Process of the fault diagnosis method.

Please cite this article as: Zhang X et al., Data-driven fault diagnosis for PEMFC systems of hybrid tram based on deep learning, International Journal of Hydrogen Energy, https://doi.org/10.1016/j.ijhydene.2020.03.035

dimension of a data set, while maintaining the feature that contributes the most to the variance of the data set [61,62].

In this paper, the original 12 - dimensional data are reduced to 4 - dimensional by PCA. As shown in Fig. 6, when the dimensionality is reduced to four, the percent variance explained is close to 90%. Therefore, the original data are replaced by the 4-dimensional data.

After PCA dimension reduction, three sets of data for each health state are listed in Table 5 as an example.

Fault samples screening

In this paper, the clustering result obtained by SAGAFCM method is used to select the fault samples. This method can make up for the shortcomings that FCM tends to converge to a local solution. As shown in Fig. 7, the objective function value converges to a smaller value through SAGAFCM method. Besides, the objective function value of SAGAFCM method converges faster.

Firstly, the 4-dimensional data after dimension reduction are marked with different types. Then four health states are obtained through SAGAFCM. According to the membership matrix got from the clustering result, the health state with the largest membership degree of each data group is seen as the label of this data group. After that, invalid data which the health state is distinct from the actual label are discarded. And the remaining data are selected as the fault samples (see Fig. 8).

Fault diagnosis

Obviously, as shown in Fig. 8, the fault samples obtained after the data preprocessing are unbalanced, especially for hydrogen leakage fault. Thus, a fault diagnosis method is proposed in this paper combined DBN and SMOTE.

The fault samples are divided into the training sample and the test sample. In order to reduce the impact of unbalanced data on classification result, SMOTE is employed to complement the small sample of the training sample. Then the new training sample is utilized to get the fault diagnosis model by training the DBN model. After that, the test sample is used to verify the accuracy of the model. In this way, the parameters in the fault diagnosis model can be continuously adjusted to get the best diagnosis model.

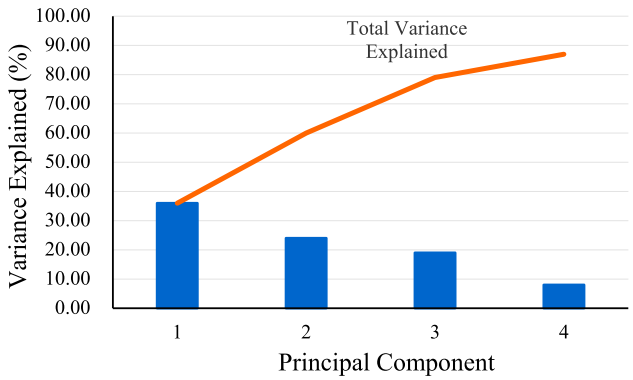

Fig. 6 – Dimension reduction by PCA.

Table 5 – Example data after PCA dimension reduction.

Fault types	Property 1	Property 2	Property 3	Property 4
N1	0.827747	0.432184	0.573878	0.173336
	0.820569	0.434626	0.571816	0.171626
	0.82469	0.445671	0.586655	0.170682
F1	0.689447	0.64806	0.571958	0.958821
	0.682223	0.647902	0.572147	0.958224
	0.68929	0.648127	0.572073	0.958742
F2	0.893979	0.382357	0.86826	0.18689
	0.877668	0.381789	0.874974	0.187217
	0.885439	0.383455	0.880768	0.188173
F3	0.900712	0.10196	0.484903	0.247334
	0.908955	0.209642	0.530314	0.223707
	0.908677	0.184406	0.479646	0.222388

Results and discussion

In this paper, the fault samples are divided into the test sample and the training sample according to the ratio of about 1:4, as shown in Table 6.

Because the data of hydrogen leakage fault are sparse, SMOTE algorithm is used to supplement the hydrogen leakage fault data in the training data before each training. And in order to get adequate training of the fault diagnosis model and guarantee the reliability of the results, this study adopts 4-fold cross-validation method. In other words, the training sample is divided into four parts on average. And three of them are used to train the model, while the remaining one is used to test the model. After each sub-sample is verified once,

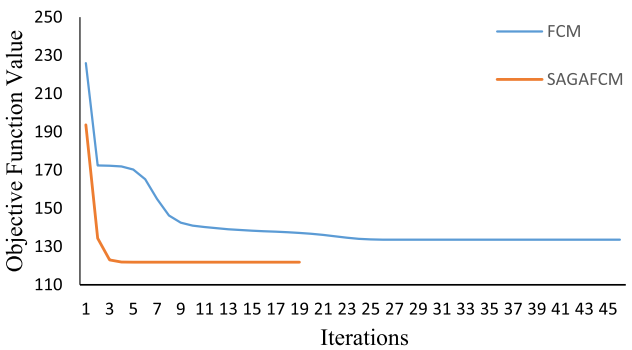

Fig. 7 – Comparison of clustering effect between FCM and SAGAFCM.

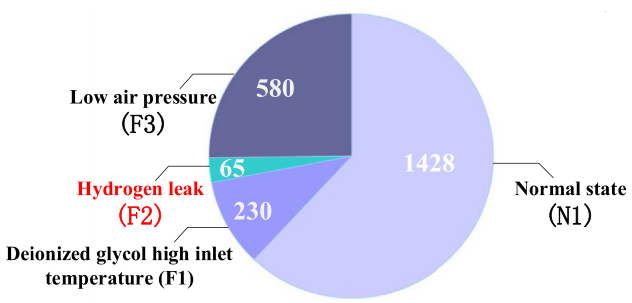

Fig. 8 – Fault samples.

Please cite this article as: Zhang X et al., Data-driven fault diagnosis for PEMFC systems of hybrid tram based on deep learning, International Journal of Hydrogen Energy, https://doi.org/10.1016/j.ijhydene.2020.03.035

the average value of the results for four times is taken as the estimation of the accuracy. Besides, in view of the randomness of the fault diagnosis algorithm and in order to ensure the reliability of the results, each accuracy is the average value obtained after running the program five times. Then the model is adjusted according to the results of the tested model, so as to get the fault diagnosis model with relatively high accuracy.

The sampling rate N in the SMOTE algorithm determines the amount of supplementary data, and the classification results vary as the sampling rate increases. The influence of different sampling rates (N) on the diagnosis accuracy is shown Fig. 9. With the increase of the sampling rate, the classification accuracy of the health states N1, F1, and F3 fluctuate little. The accuracy of N1 only decrease by less than 0.002 at most, and the accuracy of F1 has no change, though the accuracy of F3 increase, it is less than 0.01. However, the classification accuracy of F2 is obviously improved from 0.842 to 1. Besides, an excessive sampling rate can lead to the decrease in the accuracy of the four health states.

As shown in Fig. 10, the classification accuracy of the training sample has three peak points. And as compared with Fig. 9, when the sampling rate corresponds to the third peak point, the accuracy of F3 and F3 are improved without affecting the classification accuracy of other health states which means that all the health states have a good classification accuracy at this peak point. Therefore, the fault diagnosis model obtained when the sampling rate ″N = 27″ is selected as the final fault diagnosis model. And the fault diagnosis results of the training sample are shown in Table 7, when ″N = 27″, the fault diagnosis accuracy of the training sample is 99.97%, and the accuracies of N1, F1 and F3 are all 100%. And 98.844% of F2 data are correctly classified, while the rest is mistakenly classified into the normal state.

In order to show the effect of the fault diagnosis method proposed in this paper, the fault diagnosis results of the training sample by using extreme learning machine (ELM) only are compared. As shown in Fig. 11, The method proposed in this paper has obvious advantages when analyzing the big data. Compared with ELM method, this method greatly improves the classification accuracy, especially the health states of F2 and F3.

To verify the resulting fault diagnosis model, the test sample is used to test the model. As shown in Fig. 12, the classification accuracy of the four health states are all 100%. In addition, the results obtained by DBN are compared in this paper which is shown in Fig. 13, indicating that DBN combined with SMOTE can obviously improve the fault diagnosis accuracy of hydrogen leakage fault. As shown in Fig. 13, by combining SMOTE with DBN, the classification accuracy of fault F2 in the test sample is increased from 81.54% to 100%.

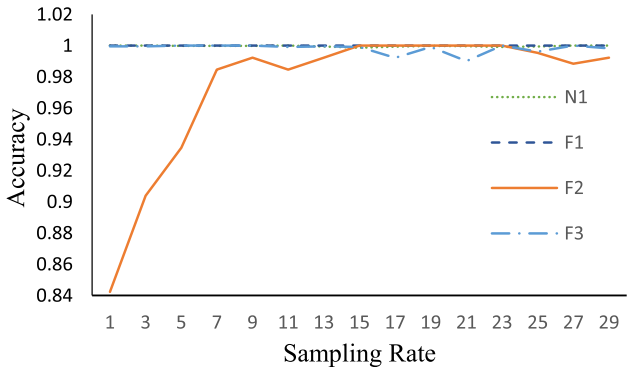

Fig. 9 – Accuracy of different health states with different sampling rates (training sample).

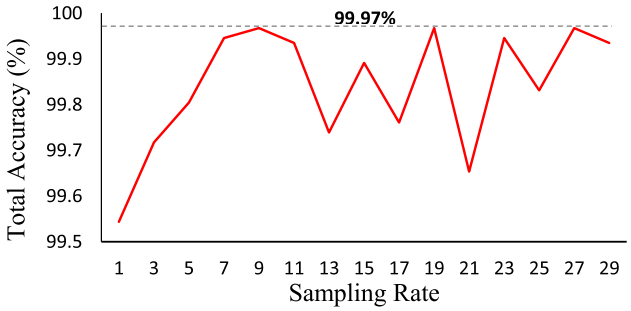

Fig. 10 – Total accuracy of different sampling rates (training sample).

Table 7 – Fault diagnosis results of the training sample when ″N = 27″.

		Diagnosed class			
		N1	F1	F2	F3
Actual class	N1	100%	0	1.16%	0
	F1	0	100%	0	0
	F2	0	0	98.84%	0
	F3	0	0	0	100%

N1: Normal state; F1: High deionized water inlet temperature fault; F2: Hydrogen leakage fault; F3: Low air pressure fault.

Conclusions

The diagnosis method proposed in this paper is a data-driven method for the PEMFC system of the hybrid tram. Considering the analysis of large amounts of data obtained by the tram operation, DBN is employed for the fault diagnosis of PEMFC systems the first time in this paper. During data

Table 6 – Sample partition of each health state.

Health state	Normal state	High deionized water inlet temperature fault	Hydrogen leakage fault	Low air pressure fault
Label	N1	F1	F2	F3
Training sample	1143	184	52	464
Test sample	285	46	13	116

Please cite this article as: Zhang X et al., Data-driven fault diagnosis for PEMFC systems of hybrid tram based on deep learning, International Journal of Hydrogen Energy, https://doi.org/10.1016/j.ijhydene.2020.03.035

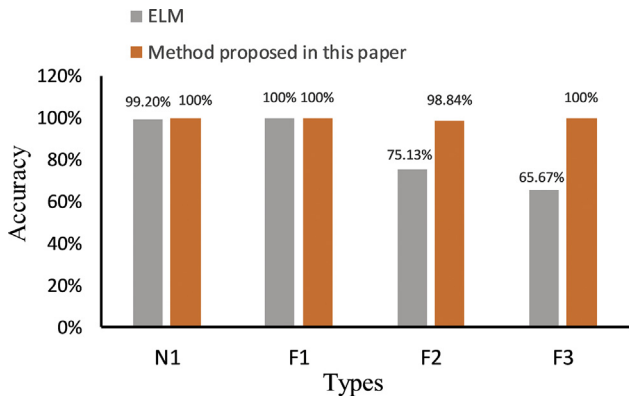

Fig. 11 – Fault diagnosis results of the proposed method and ELM (training sample).

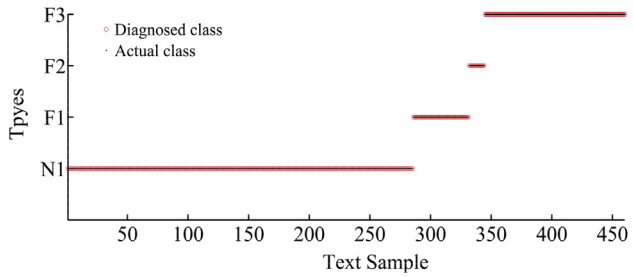

Fig. 12 – Fault diagnosis results of the test sample.

preprocessing, redundant and invalid data in the collected original data are discarded by SAGAFCM method, so as to obtain the fault samples which are divided into the training sample and the test sample. And considering the influence of the unbalanced fault samples on the fault diagnosis accuracy, SMOTE algorithm is employed to supplement the small sample data in the training sample, forming the new training sample to train the DBN model.

In this paper, high deionized water inlet temperature fault, hydrogen leakage fault, low air pressure fault and the normal state of the PEMFC system are classified by the proposed method. The results show that this method can effectively process the large amount of data on the tram. And an excellent fault classification effect can be obtained by the proposed method with the accuracy of the training sample reaching 99.97%, and the accuracy of the test sample reaching 100%.

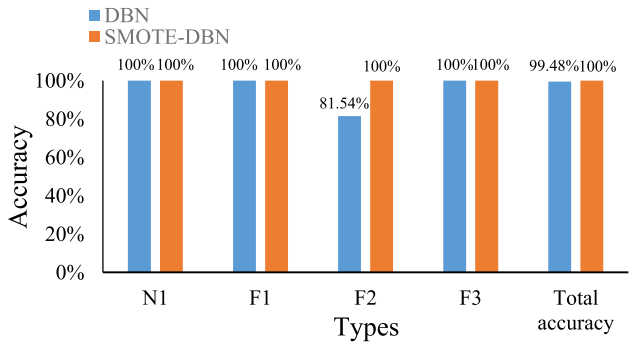

Fig. 13 – Fault diagnosis results of DBN and DBN combined with SMOTE (test sample).

The comparison with ELM method shows that this method has good classification results when analyzing large amounts of data. Moreover, through the combination of SMOTE and DBN, the results show that the classification accuracy of the small sample in fault samples can be greatly improved by adjusting the sampling rate.

This method is suitable for the fault diagnosis of large sample data, and has a good effect when analyzing unbalanced data. Besides, this method can provide the reference for realizing the control strategy online of the fuel cell system on the tram.

Acknowledgements

This work is supported by the National Natural Science Foundation (No. 51607149), Department of Science and Technology of Sichuan Province (No. 2019YJ0236), Foundation of Key Laboratory of Magnetic Suspension Technology and Maglev Vehicle, Ministry of Education.

REFERENCES

[1] Chen HC, Xu SC, Pei PC, Qu BW, Zhang T. Mechanism analysis of starvation in PEMFC based on external characteristics. Int J Hydrogen Energy 2019;44(11):5437–56. https://doi.org/10.1016/j.ijhydene.2018.11.135.

[2] Lin RH, Xi XN, Wang PN, Wu BD, Tian SM. Review on hydrogen fuel cell condition monitoring and prediction methods. Int J Hydrogen Energy 2019;44(11):5488–98. https://doi.org/10.1016/j.ijhydene.2018.09.085.

[3] Wang JY. Barriers of scaling-up fuel cells: cost, durability and reliability. Energy 2015;80:509–21. https://doi.org/10.1016/j.energy.2014.12.007.

[4] Dubau L, Castanheira L, Maillard F, Chatenet M, Lottin O, Maranzana G, et al. A review of PEM fuel cell durability: materials degradation, local heterogeneities of aging and possible mitigation strategies. Wiley Interdiscipl Rev Energy Environ 2014;3(6):540–60. https://doi-org-s.era.lib.swjtu.edu.cn/10.1002/wene.113.

[5] Muhammad FC, Jaeseung L, Hyunchul J. Numerical study for diagnosing various malfunctioning modes in PEM fuel cell systems. Int J Hydrogen Energy , Available online 10 August 2019. https://doi.org/10.1016/j.ijhydene.2019.07.126.

[6] Mohammadi A, Djerdir A, Steiner NY, Khaburi D. Advanced diagnosis based on temperature and current density distributions in a single PEMFC. Int J Hydrogen Energy 2015;40(45):15845–55. https://doi.org/10.1016/j.ijhydene.2015.04.157.

[7] Chen CY, Huang KP, Yan WM, Lai MP, Yang CC. Development and performance diagnosis of a high power air-cooled PEMFC stack. Int J Hydrogen Energy 2016;41(27):11784–93. https://doi.org/10.1016/j.ijhydene.2015.12.202.

[8] Wang H, Gaillard A, Hissel D. Online electrochemical impedance spectroscopy detection integrated with step-up converter for fuel cell electric vehicle. Int J Hydrogen Energy 2019;44(2):1110–21. https://doi.org/10.1016/j.ijhydene.2018.10.242.

[9] Suresh R, Swaminathan S, Rengaswamy R. Rapid impedance spectroscopy using dual phase shifted chirp signals for electrochemical applications. Int J Hydrogen Energy 2020;45(17):10536–48. https://doi.org/10.1016/j.ijhydene.2019.10.031.

[10] Mao L, Jackson L, Davies B. Investigation of PEMFC fault diagnosis with consideration of sensor reliability. Int J Hydrogen Energy 2018;43(35):16941–8. https://doi.org/10.1016/j.ijhydene.2017.11.144.
[11] Li A, Aitouche A, Wang H, Christov N. Sensor fault estimation of PEM fuel cells using Takagi Sugeno fuzzy model. Int J Hydrogen Energy 2020;45(19):11267–75. https://doi.org/10.1016/j.ijhydene.2019.01.100.
[12] Bougatef Z, Abdelkrim N, Aitouche A, Abdelkrim MN. Fault detection of a PEMFC system based on delayed LPV observer. Int J Hydrogen Energy 2020;45(19):11233–41. https://doi.org/10.1016/j.ijhydene.2018.11.053.
[13] Liu JX, Luo WS, Yang XZ, Wu LG. Robust model-based fault diagnosis for PEM fuel cell air-feed system. IEEE Trans Ind Electron 2016;65(5):3261–9. https://doi.org/10.1109/TIE.2016.2535118.
[14] Xie CJ, Xu XY, Bujlo P, Shen D, Zhao HB, Zhao HB. Fuel cell and lithium iron phosphate battery hybrid powertrain with an ultracapacitor bank using direct parallel structure. J Power Sources 2015;279:487–94. https://doi.org/10.1016/j.jpowsour.2015.01.029.
[15] Benmouna A, Becherif M, Depernet D, Gustin F, Ramadan HS, Fukuhara S. fault diagnosis methods for proton exchange membrane fuel cell system. Int J Hydrogen Energy 2017;42(2):1534–43. https://doi.org/10.1016/j.ijhydene.2016.07.181.
[16] Petrone R, Zheng Z, Hissel D, Pera MC, Pianese C, Sorrentino M, et al. A review on model-based diagnosis methodologies for PEMFCs. Int J Hydrogen Energy 2013;38(17):7077–91. https://doi.org/10.1016/j.ijhydene.2013.03.106.
[17] de Lira S, Puig V, Quevedo J. Robust LPV model-based sensor fault diagnosis and estimation for a PEM fuel cell system. In: Conference on control and fault-tolerant systems, Nice, France; 2010. p. 819–24. https://doi.org/10.1109/SYSTOL.2010.5676000.
[18] Polverino P, Frik E, Jung D, Krysander M, Pianese C. Model-based diagnosis through structural analysis and causal computation for automotive polymer electrolyte membrane fuel cell systems. J Power Sources 2017;347:26–40. https://doi.org/10.1016/j.jpowsour.2017.04.089.
[19] Mohammadi A, Cirrincione G, Djerdir A, Khaburi D. A novel approach for modeling the internal behavior of a PEMFC by using electrical circuits. Int J Hydrogen Energy 2018;43(25):11539–49. https://doi.org/0.1016/j.ijhydene.2017.08.151.
[20] Taleb MA, Bethoux O, Godoy E. Identification of a PEMFC fractional order model. Int J Hydrogen Energy 2017;42(2):1499–509. https://doi.org/10.1016/j.ijhydene.2016.07.056.
[21] Zheng Z, Petrone R, Pera MC, Hissel D, Becherif M, Pianese C, et al. A review on non-model based diagnosis methodologies for PEM fuel cell stacks and systems. Int J Hydrogen Energy 2013;38(21):8914–26. https://doi.org/0.1016/j.ijhydene.2013.04.007.
[22] Benouioua D, Candusso D, Harel F, Oukhellou L. PEMFC stack voltage singularity measurement and fault classification. Int J Hydrogen Energy 2014;39(36):21631–7. https://doi.org/10.1016/j.ijhydene.2014.09.117.
[23] Benouioua D, Candusso D, Harel F, Picard P, François X. On the issue of the PEMFC operating fault identification: generic analysis tool based on voltage pointwise singularity strengths. Int J Hydrogen Energy 2018;43(25):11606–13. https://doi.org/10.1016/j.ijhydene.2017.09.177.
[24] Zheng ZX, Péra MC, Hissel D, Becherif M, Agbli KS, Li YD. A double-fuzzy diagnostic methodology dedicated to online fault diagnosis of proton exchange membrane fuel cell stacks. J Power Sources 2014;271:570–81. https://doi.org/10.1016/j.jpowsour.2014.07.157.
[25] Costamagna P, De Giorgi A, Moser G, Serpico SB, Trucco A. Data-driven techniques for fault diagnosis in power generation plants based on solid oxide fuel cells. Energy Convers Manag 2019;180:281–91. https://doi.org/10.1016/j.enconman.2018.10.107.
[26] Zhao XW, Xu LF, Li JQ, Fang C, Ouyang MG. Faults diagnosis for PEM fuel cell system based on multi-sensor signals and principle component analysis method. Int J Hydrogen Energy 2017;42(29):18524–31. https://doi.org/10.1016/j.ijhydene.2017.04.146.
[27] Lin RH, Pei ZX, Ye ZZ, Guo CC, Wu BD. Hydrogen fuel cell diagnostics using random forest and enhanced feature selection. Int J Hydrogen Energy 2020;45(17):10523–35. https://doi.org/10.1016/j.ijhydene.2019.10.127.
[28] Li ZL, Outbib R, Giurgea S, Hissel D, Giraud A, Couderc P. Fault diagnosis for fuel cell systems: a data-driven approach using high-precise voltage sensors. Renew Energy 2019;135:1435–44. https://doi.org/10.1016/j.renene.2018.09.077.
[29] Li ZL, Outbib R, Giurgea S, Hissel D. fault diagnosis for PEMFC systems in consideration of dynamic behaviors and spatial inhomogeneity. IEEE Trans Energy Convers 2019;34(1):3–11. https://doi.org/10.1109/TEC.2018.2824902.
[30] Li ZL, Cadet C, Outbib R. Diagnosis for PEMFC based on magnetic measurements and data-driven approach. IEEE Trans Energy Covers 2019;34(2):964–72. https://doi.org/10.1109/TEC.2018.2872118.
[31] Zhou S, Dhupia JS. Online adaptive water management fault diagnosis of PEMFC based on orthogonal linear discriminant analysis and relevance vector machine. Int J Hydrogen Energy 2019;45(11):7005–14. https://doi.org/10.1016/j.ijhydene.2019.12.193.
[32] Liu JW, Li Q, Chen WR, Cao TQ. A discrete hidden Markov model fault diagnosis strategy based on K-means clustering dedicated to PEM fuel cell systems of tramways. Int J Hydrogen Energy 2018;43(27):12428–41. https://doi.org/10.1016/j.ijhydene.2018.04.163.
[33] Zheng ZX, Morando S, Pera MC, Hissel D, Larger L, Martinenghi R, et al. Brain-inspired computational paradigm dedicated to fault diagnosis of PEM fuel cell stack. Int J Hydrogen Energy 2017;42(8):5410–25. https://doi.org/10.1016/j.ijhydene.2016.11.043.
[34] Liu JW, Li Q, Yang HQ, Han Y, Jiang SN, Chen WR. Sequence fault diagnosis for PEMFC water management subsystem using deep learning with t-SNE. IEEE Access 2019;7:92009–19. https://doi.org/10.1109/ACCESS.2019.2927092.
[35] Zhang ZH, Li SH, Xiao YW, Yang YP. Intelligent simultaneous fault diagnosis for solid oxide fuel cell system based on deep learning. Appl Energy 2019;233–234:930–42. https://doi.org/10.1016/j.apenergy.2018.10.113.
[36] Hinton G, Osindero S, Teh YW. A fast learning algorithm for deep belief nets. Neural Comput 2006;18(7):1527–54. https://doi.org/10.1162/neco.2006.18.7.1527.
[37] Chen CLP, Zhang CY, Chen L, Gan M. Fuzzy Restricted Boltzmann Machine for the enhancement of deep learning. IEEE Trans Fuzzy Syst 2015;23(6):2163–73. https://doi.org/10.1109/TFUZZ.2015.2406889.
[38] Ranzato M, Susskind J, Mnih V, Hinton G. On deep generative models with applications to recognition. In: 2011 IEEE conference on computer vision and pattern recognition(CVPR), Colorado Springs, CO, USA; 2011. p. 2857–64.
[39] Sanjanaashree P, Anand KM. Joint layer based deep learning framework for bilingual machine transliteration. In: 2014 international conference on advances in computing,

Please cite this article as: Zhang X et al., Data-driven fault diagnosis for PEMFC systems of hybrid tram based on deep learning, International Journal of Hydrogen Energy, https://doi.org/10.1016/j.ijhydene.2020.03.035

communications and informatics (ICACCI), New Delhi; 2014. p. 1737–43.
[40] Wang X, Li Y, Rui T, Zhu HJ, Fei JC. Bearing fault diagnosis method based on Hilbert envelope spectrum and deep belief network. J Vibroeng 2015;17(3):1295–308.
[41] Chen ZY, Zeng XQ, Li WH, Liao GL. Machine fault classification using deep belief network. In: 2016 IEEE international instrumentation and measurement technology conference proceedings, taipei; 2016. p. 1–6.
[42] Shen CQ, Xie JQ, Wang D, Jiang XX, Shi JJ, Zhu ZK. Improved hierarchical adaptive deep belief network for bearing fault diagnosis. Appl Sci-Basel 2019;9(16):3374. https://doi.org/10.3390/app9163374.
[43] Zhao HM, Liu HL, Xu JJ, Guo C, Deng W. Research on a fault diagnosis method of rolling bearings using variation mode decomposition and deep belief network. J Mech Sci Technol 2019;33(9):4165–72. https://doi.org/10.1007/s12206-019-0811-2.
[44] Zhang TF, Li Z, Deng ZH, Hu B. Hybrid data fusion DBN for intelligent fault diagnosis of vehicle reducers. Sensors 2019;19(11):2504. https://doi.org/10.3390/s19112504.
[45] Tamilselvan P, Wang Y, Wang P. Deep Belief Network based state classification for structural health diagnosis. In: 2012 IEEE aerospace conference, big sky, MT; 2012. p. 1–11.
[46] Yan Yu, Li Q, Chen WR, Su B, Liu JW, Ma L. Optimal energy management and control in multimode equivalent energy consumption of fuel cell/supercapacitor of hybrid electric tram. IEEE Trans Ind Electron 2019;66(8):6065–76. https://doi.org/10.1109/TIE.2018.2871792.
[47] Li Q, Chen W, Liu Z, Guo A, Huang J. Nonlinear multivariable modeling of locomotive proton exchange membrane fuel cell system. Int J Hydrogen Energy 2014;39(25):13777–86. https://doi.org/10.1016/j.ijhydene.2013.12.211.
[48] Zhao Q, Shao S, Lu LX, Liu X, Zhu HL. A new PV array fault diagnosis method using fuzzy c-mean clustering and fuzzy membership algorithm. Energies 2018;11(1):238. https://doi.org/10.3390/en11010238.
[49] Suprihatin, Yanto ITR, Irsalinda N, Purwaningsih T, Haviluddin, Wibawa AP. A performance of modified fuzzy C-means (FCM) and chicken swarm optimization (CSO). In: 3rd international conference on science in information technology (ICSITech), Bandung; 2017; 2017. p. 171–5.
[50] Guo PF, Wang XZ, Han YS. The enhanced genetic algorithms for the optimization design. In: 2010 3rd international conference on biomedical engineering and informatics, Yantai; 2010. p. 2990–4.
[51] Tang XH, Chang X, Fang ZF. A multi-objective genetic algorithm based on simulated annealing. In: 2012 fourth international conference on multimedia information networking and security, Nanjing; 2012. p. 413–6.
[52] Ariza HE, Correcher A, Sanchez C, Perez-Navarro A, Garcia E. Thermal and electrical parameter identification of a proton exchange membrane fuel cell using genetic algorithm. Energies 2018;11(8):2099. https://doi.org/10.3390/en11082099.
[53] Chen XY. Research on network optimization based on simulated annealing genetic algorithm. In: 5th international conference on machinery, materials and computing technology (ICMMCT), Beijing; 2017. p. 1349–54.
[54] Arel I, Rose DC, Karnowski TP. Deep machine learning-A new frontier in artificial intelligence research. IEEE Comput Intell Mag 2010;5(4):13–8. https://doi.org/10.1109/MCI.2010.938364.
[55] Tamilselvan P, Wang PF. Failure diagnosis using deep belief learning based health state classification. Reliab Eng Syst Saf 2013;115:124–35. https://doi.org/10.1016/j.ress.2013.02.022.
[56] Hinton GE. Training products of experts by minimizing contrastive divergence. Neural Comput 2002;14(8):1771–800. https://doi.org/10.1162/089976602760128018.
[57] Xu J, Liu C. Transformer fault diagnosis using restricted Boltzmann machines. Comput Sci Theory Methods 2017:682–8.
[58] Tran VT, Tran VT, Tinga T, Ball A, Niu G. Single and combined fault diagnosis of reciprocating compressor valves using a hybrid deep belief network. Proc Inst Mech Eng Part C-J Eng Mech Eng Sci 2018;232(20):3767–80. https://doi.org/10.1177/0954406217740929.
[59] Wang J, Yun B, Huang PL, Liu YA. Applying threshold SMOTE algorithm with attribute bagging to imbalanced datasets. In: 8th international conference on rough sets and knowledge technology (RSKT), Halifax; 2013. p. 221–8.
[60] Liu JW, Li Q, Chen WR, Yan Y, Wang XT. A fast fault diagnosis method of the PEMFC system based on extreme learning machine and dempster-shafer evidence theory. IEEE Trans Transport Electr 2019;5(1):271–84. https://doi.org/10.1109/TTE.2018.2886153.
[61] Hua JF, Li JQ, Ouyang MG, Lu LG, Xu LF. Proton exchange membrane fuel cell system diagnosis based on the multivariate statistical method. Int J Hydrogen Energy 2011;36(16):9896–905. https://doi.org/10.1016/j.ijhydene.2011.05.075.
[62] Placca L, Kouta R, Candusso D, Blachot JF, Charon W. Analysis of PEM fuel cell experimental data using principal component analysis and multi linear regression. Int J Hydrogen Energy 2010;35(10):4582–91. https://doi.org/10.1016/j.ijhydene.2010.02.076.

Please cite this article as: Zhang X et al., Data-driven fault diagnosis for PEMFC systems of hybrid tram based on deep learning, International Journal of Hydrogen Energy, https://doi.org/10.1016/j.ijhydene.2020.03.035